Nature Environment and Pollution Technology
An International Quarterly Scientific Journal

p-ISSN: 0972-6268
(Print copies up to 2016)
e-ISSN: 2395-3454

Vol. 20 | No. 2 | pp. 467-479 | 2021

Original Research Paper

https://doi.org/10.46488/NEPT.2021.v20i02.003

Open Access Journal

Adsorption of Dyes by Chitosan-Selenium Nanoparticles: Recent Developments and Adsorption Mechanisms

John Britto, P. Barani, M. Vanaja, E. Pushpalaksmi, J. Jenson Samraj and G. Annadurai†
Division of Nanoscience, Sri Paramakalyani Centre for Excellence in Environmental Sciences, Manonmaniam Sundaranar University, Alwarkurichi-627 412, India
†Corresponding author: G. Annadurai; gannadurai@msuniv.ac.in

Nat. Env. & Poll. Tech.
Website: www.neptjournal.com

Received: 27-05-2020
Revised: 08-07-2020
Accepted: 25-07-2020

Key Words:
Rhodamine
Chitosan-selenium nanoparticles
Langmuir isotherm
Justicia adhatoda

ABSTRACT

Most of the dyes are a dangerous class of water contaminants that have affected the environment drastically. Nano-sized compositeis the best decision cutting edge adsorbent for the evacuation of water poisons as such materials are related to the attributes of straightforwardness, adaptability, adequacy, and high surface reactivity. In this investigation, we have synthesized a nanostructured Chitosan-Selenium nanoparticle by green synthesis method using *Justicia adhatoda* plant leaves extract. Synthesis and characterization of Chitosan-Selenium nanoparticle were described by UV-visible spectroscopy, FTIR spectrum examinations, Particle Size Analysis, and XRD Spectrum analysis. From the outcomes, it was inferred that the Chitosan-Selenium nanoparticle was additionally utilized as an adsorbent for the expulsion of Rhodamine dye from the aqueous solution. Langmuir isotherm model was effectively usedfor the adsorption study of Chitosan-Selenium nanoparticle adsorbent. For the adsorption studies, parameters such asdosages, pH, and temperature were studied. The adsorption process was remarkably fast and reached equilibrium within 24hrs. The isotherm information was steady with the Langmuir model, and the most extreme adsorption limits of the Chitosan-Selenium nanoparticle adsorbent was 34.5mg.g^{-1} for Rhodamine dye. Accordingly, nanoparticleswill be the only wayfor the future planned water treatment process.

INTRODUCTION

Industrial, agricultural and domestic wastes, due to the rapid development in technology, are discharged in several environments. Generally, this discharge is directed to the nearest water sources such as rivers, lakes, and seas. The textile dyeing process is an important source of contamination responsible for the continuous pollution of the environment. Textile, paper, painting, and coating industries are majorsources of dye pollutants. A large amount of dye wastewateris emptied into freshwater bodies which have negativeconsequences on the environment and human health (Oliveiraet al. 2008). Wastewater from dye-stuff and textile industries have dye concentrations below 1 g/dm^3, high alkalinity, Biochemical Oxygen Demand (BOD), Chemical Oxygen Demand (COD), and total dissolved solids (Kaushik & Malik 2009). The reactive, directive, and acid dye widely used in silk, cotton, and wool processing as dyes (El-Sharkawy et al. 2007). Dye wastewater that ends up in freshwater bodies causes havoc to aquatic species by increasing toxicity in COD. It also affects the photosynthetic activities of aquatic plants through the reduction of light penetration (Oliveira et al. 2008). It has been reported that high COD,BOD values, particulate matter (PM) and sediments, grease, and oil in effluents lead to the depletion of dissolved oxygen creating serious consequences on aquatic species (Wang et al. 2011, Hamza & Hamoda 1980, Shaul et al. 1982, Shelley et al. 1980). The methods of colour removal from industrial effluents include biological treatment, coagulation, flotation, adsorption, oxidation, and hyperfiltration. Among the treatment options, adsorption has become one of the most effective and comparable low-cost methods for the decolourization of textile wastewater. Different adsorbents have been used for the removal from aqueous solutions of various materials, such as dyes, metal ions, and other organic materials include perlite (Dogan et al. 2000, Demirbas & Dogan 2002, Dogan & Alkan 2003) bentonite (Bereket et al. 1997), silica gels (Mohamed et al. 1996), fly ash (Mohan et al. 2002, Gupta et al. 2000), lignite (Allen et al. 1989), peat (Ho& Mckay 1998), silica (Mckay et al. 1981). However, all these processes are costly and cannot be used by small industries to treat a wide range of dye wastewater (Dogan et al. 2000). The adsorption process provides an attractive alternative for the treatment of contaminated waters, especially if the sorbent is inexpensive and does not require an additional pretreatment step before its application (Mckay et al. 1981, Ho & Mckay

1998,Ashraf 2016, Nurchi et al. 2014, Chang et al. 2014, Arica et al. 2017, 2019, Bayramoglu et al. 2012,Bayramoglu & Yilmaz 2018). A wide range of nanomaterials such as metals, metal oxide, polymer composites, and nanoparticles incorporating activated carbon, biomass, and clay minerals, etc. have been included. Adsorption requires less land area, least effect to toxic chemicals, greater flexibility in the design, and operation and superior removal of organic contaminants. Therefore, significant attention has been directed to adsorption as a process for colour removal from wastewaters since it offers the most economical and effective treatment methods. Therefore, adsorption became one of the most effective methods to remove the colour from textile wastewater. The objective of this paper was to explore the removal of Rhodamine dye in an aqueous solution by adsorption on the Chitosan-Selenium nanoparticle. The influence of several parameters on adsorption such as dosages, pH, and temperature on the adsorption process was also studied.

MATERIALS AND METHODS

Chemicals and Collection of Plant Material

All the chemicals were purchased from Himedia Private Ltd, Mumbai. The plant *Justicia adhatoda* leaves were collected from Sri Paramakalyani Centre of Excellence in Environmental Sciences, Manonmaniam Sundaranar University, Alwarkurichi.

Preparation of Adathoda Leaf Extract

Fresh and young leaves (5g) of the Adathoda plant were washed thoroughly with distilled water and cut into fine pieces. Leaves were subsequently macerated in 20 mL of Tris-HCl (pH7.5) with the help of mortar and pestle. A thick slurry of leaf thus recovered was subjected to centrifugation at 10,000 rpm for 5 min at 4°C. The supernatant was transferred into fresh sterile centrifuge tubes followed by its preservation in refrigerated conditions. The aqueous extract of leaf obtained in this manner was used as a precursor for the synthesis of selenium nanoparticles.

Synthesis of Selenium Nanoparticle

In a typical synthesis of selenium nanoparticles, the leaf extract (2 mL) which contains dissolved phytochemicals was added dropwise into 20 mL of sodium selenite solution (10mM). The addition of the leaf extract was carried out under magnetic stirring. The content was later on placed on to a rotator orbital shaker operating at 200rpm for 24 h. The incubation of the mixture was performed at 30°C in dark conditions. The reduction of selenium ions was monitored by sampling an aliquot (3 mL) of the mixture at intervals of 12 h, followed by measurement of the UV-Vis spectrophotometer. To find out the absorption maximum, a spectral scanning analysis was carried out by measuring the optical density of the content from wavelength 250 to 750 nm.

Synthesis of Chitosan-Selenium Nanoparticle (CS-Se NPs)

Stock solutions of sodium selenite (20mmol/L) and ascorbic acid solution (80mmol/L) were prepared with double-distilled water at room temperature. 1 gm of chitosan (CS, 1% w/w) was dispersed in 4% (w/w) acetic acid at room temperature and stirred for complete dissolution. For the preparation of the CS-Se NPs solution, 1mL (10 mM) of sodium selenite solution, ascorbic acid, and chitosan solution were mixed and the solution was subjected to vigorous mixing. Then, the reaction mixture was diluted to 10 mL with distilled water. The sample was filtered and dried in the hot air oven at 150°C for using adsorption studies.

Batch Equilibrium Studies

Batch adsorption experiments were carried out by agitating 1g of the Chitosan-Selenium nanoparticle with the effect of initial Rhodamine dye concentrations was carried out by shaking 100 mLRhodamine dye solutions of desired concentrations (20 to 100 mg/L) with 1g of the adsorbent at different dosages (1.0, 2.0 and 3.0g/L) pH (5.8, 6.8 and 9.4) and temperature (30°C, 45°C, and 60°C) using an orbital shaker operating at 200 rpm. Before the measurement of colour, the dye solutions were filtered through Whatman No. 1 filter paper to exclude the adsorbent particles. Dye concentrations were measured at the wavelengths corresponding to their maximum absorbance using a spectrophotometer. The effect of pH was studied by adjusting the pH of dye solutions using 1 N H_2SO_4 or 1 N NaOH solution pH was measured using a pH meter. The samples were withdrawn from the shaker at a pre-determined time of 24hrs. The residual concentrations of Rhodamine dye were measured using UV spectrophotometer equipment (Shimadzu UV/Vis 1601 Spectrophotometer, Japan). The maximum wavelength of this dye is λ_{max}555 nm.

Mass Balance Equation

Throughout the experiment the mass balance equation was used, to find the amount of protein adsorbed in each flask which was determined by the equation,

$$Q = V (C_o - C_e)/W \quad \text{... (1)}$$

Where,

Q - Adsorption capacity (mg/g)

C_o - Initial concentration of Rhodamine dye (mg/L)

C_e - Final concentration of Rhodamine dye(mg/L)

V - Solution volume of Rhodamine dye (L)

W - Mass of adsorbent (g)

So using this equation the amount of dye being adsorbed by the adsorbent was determined.

RESULTS AND DISCUSSION

The synthesis of selenium nanoparticles was preliminarily analysed by the colour change of the reaction mixture. The reaction mixture contains sodium selenite solution, ascorbic acid, and plant extract. The plant extract was used as a reducing agent forthe synthesis of nanoparticles. Ascorbic acid was used as an initiator of the reduction reaction. All the solutions were mixed and colour change was occurring from colourless sodium selenite solution to ruby red colour. A similar result was observed by Kirupagaran et al.(2016), synthesized selenium nanoparticles using an extract of *Leucas lavandulifolia* and Fenugreek seed extract (Ramamurthy et al. 2013). Visual observation of the chitosan stabilized selenium nanoparticles solution showed a colour change from light yellow to brick red indicating the formation of red-coloured elemental Se resulting in the selenium nanoparticle formation (Bajaj et al. 2012). This red colour due to the excitation of surface plasmon vibrations of selenium nanoparticles provides a convenient spectroscopic signature of their production whereas no colour change could be demonstrated in a solution of selenium selenite as a negative control. Many related studies revealed that metal reduction and precipitation might involve a complex of either reductase, capping proteins, quinones or cytochromes, electron shuttles, or phytochelatins that are known to reduce and stabilize various metal, metal oxides and metal sulphide nanoparticles (Bajaj et al. 2012).

UV-Vis Spectrophotometer

Reduction of selenium ions into selenium nanoparticles during exposure to plant extracts and ascorbic acid was observed using UV-Vis spectra. The metal nanoparticles have free electrons, which give the SPR absorption band, due to the combined vibration of electrons of metal nanoparticles. Chitosan stabilized selenium nanoparticles shown the SPR band at 450 and 310 nm indicates the formation of selenium nanoparticles. Some of the minor peaks were also observed due to the presence of biomolecules from chitosan Fig.1. Previous studies have shown that the spherical Se-NPs contribute to the absorption bands at around 250-400nm in the UV-Visible spectra (Fesharaki et al. 2010) reported λ_{max} at 280 nm (Lin et al. 2005) at 355 nm (Shen et al. 2000) at 380 nm. The UV data may support further characterization of *Adhatoda* leaf extract and chitosan mediated selenium

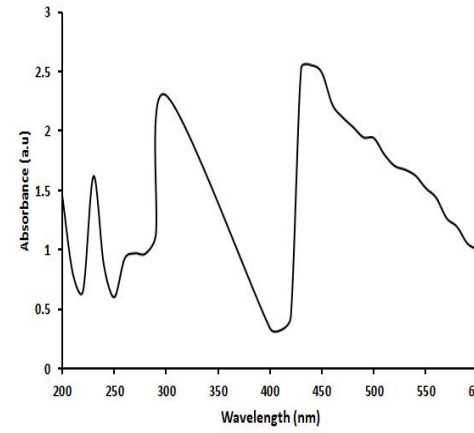

Fig. 1: UV-Vis spectra of chitosan mediated synthesized selenium nanoparticles.

nanoparticles. Chitosan stabilized selenium nanoparticles were purified by membrane dialysis process. Dialysed nanoparticles were dried in a hot air oven at 60°C for 4 h. The powder form of the selenium nanoparticles was used for further analysis.

FT-IR Analysis

The functional groups present in green synthesized chitosan-selenium nanoparticles were identified by FTIR spectra. FTIR analysed at different wavenumber range from 4000 to 500cm^{-1}. The functional groups involved in the synthesis of selenium nanoparticles using chitosan were detected with the help of FT-IR analysis (Fig. 2). Broadband at 3226cm^{-1} was observed due to the presence of O-H stretching carboxylic acids. A very small band at 2878 cm^{-1} was formed corresponds to C-H stretch alkanes. A strong narrowband was positioned at N-H bend primary amines. A small band at 1297 cm^{-1} indicates the presence of N-O symmetric stretching Nitro compounds and C-N stretching aromatic amines. A narrow band was formed at 1023 due to C-N

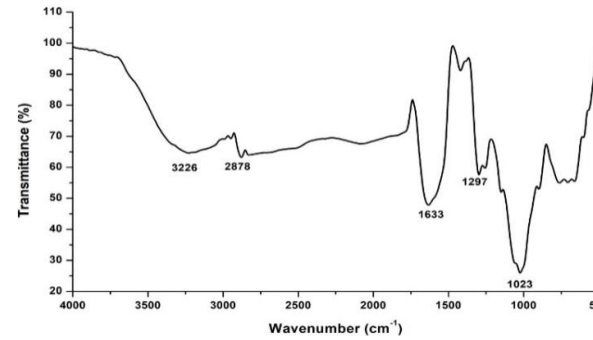

Fig. 2: FTIR spectrum of chitosan-selenium nanoparticles.

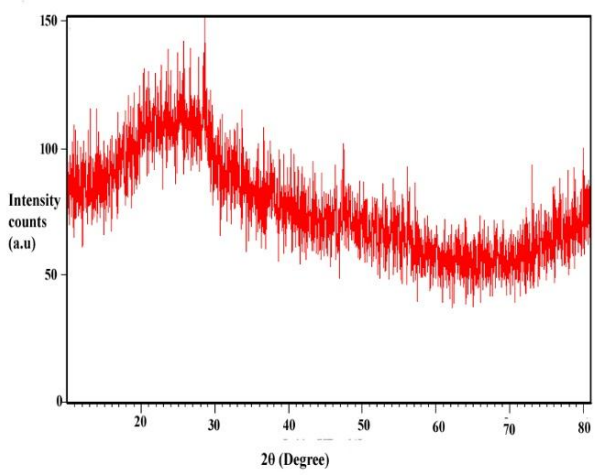

Fig. 3: XRD Spectrum of the chitosan-selenium nanoparticle.

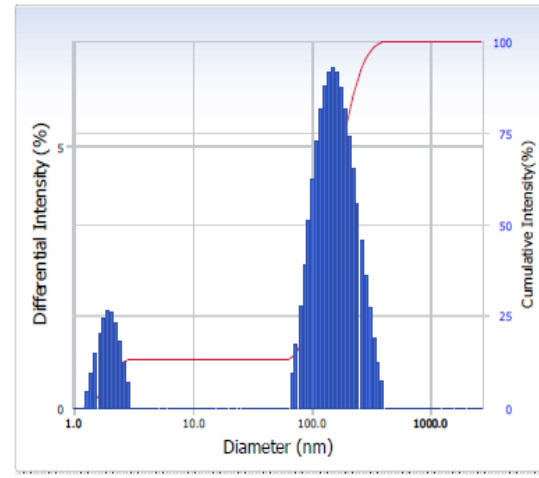

Fig. 4: Particle size analysis of chitosan-selenium nanoparticles.

stretch aliphatic amines. Therefore, the FT-IR results imply that the chitosan-selenium nanoparticles were successfully synthesized and capped with bio-compounds present in the leaf aqueous extract and chitosan by using a green method.

X-ray Diffraction

The crystal structure and the phase composition of chitosan-selenium nanoparticles were determined, using XRD techniques shown in Fig. 3. The XRD pattern suggests that the sample is nanocrystalline and matches very well with that of the standard selenium powder confirming the formation of selenium particles using leaf extract. The calculated lattice constants are a = 4.363 A° and c = 4.952 A° which are in agreement with the literature value (JCPDS File No.06-0362). The clear peaks of cubic phases at 23.68, 29.12, 40.71, 45.24, 48.05, and 51.28° were assigned to (100), (101), (110), (111), (200) and (201) crystalline planes which may be due to the presence of additional bioactive compounds present in the *Adathoda* leaf extract (Shen et al. 2000). Chitosan coupled selenium nanoparticles not shown specific crystalline planes and definite shapes indicate that synthesized nanocomposite is a polydispersed amorphous structure.

Particle Size Analysis

Fig. 4. shows the number of frequency histograms of particle size data on a linear scale. The smooth curve drawn through the histogram is a valid size-frequency curve insufficient particle-sare counted and the size interval is at least ten (Kirupagaran et al. 2016). As it is observed in Fig. 4 the average size distribution of the chitosan-selenium nanoparticle is 87-152 nm.

Adsorption Isotherm of Rhodamine Dye

The equilibrium adsorption isotherm is of fundamental importance in the design of adsorption systems. The isotherm expresses the relation between the mass of dye adsorbed at a particular temperature and dosages and the liquid phase of dye concentration. For any adsorption investigation one of the most important parameters required to understand the behaviour of the adsorption process in the adsorption isotherm (Jain et al. 2003, Jumasiah et al. 2005, Kadirvelu et al. 2005, Kamel et al. 2009). The shape of an isotherm not only provides information about the affinity of the dye molecule for adsorption but also reflects the possible mode of adsorbing dye molecule. The most common way of obtaining an adsorption isotherm is to determine the concentration of dye solution before and after the adsorption experiments, although several attempts have been made to find the adsorbed amount.

Effect of Dosages

The effect of adsorbent dosages on Rhodamine dye uptakes for three different dosages (Chitosan-Selenium Nanoparticle) (1.0, 2.0, and 3.0 g/L) is shown in Fig. 5. It can be observed that as the dosages were increased, the adsorption of dye increases. The results show that there is a gradual increase in adsorption with increasing dosages. Such an effect of probably due to the inability of the large dye molecule to penetrate all the internal pore structure Chitosan-Selenium nanocomposite and a similar phenomenon was reported previously for the adsorption of certain dyes on various adsorbents (Mckay 1984. Feng et al. 2001. Ferrero 2000). The results revealed that the dye uptake increased with increasing dosages at1.0 g/L 16.14 mg/g. 2.0g/L, 24.36.0 mg/g and 3.0g/L, 33.90 mg/g). This is due to the larger surface area made available for adsorption. It was also observed that the increase in dosages, increases the dye

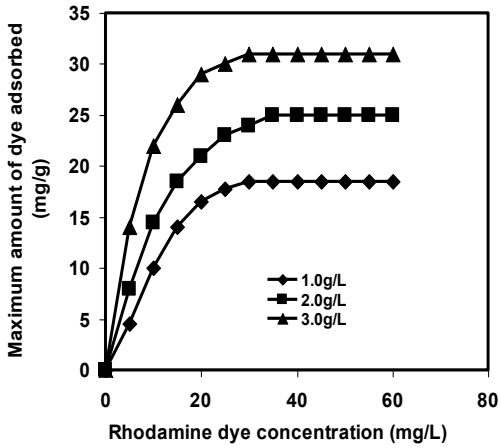

Fig. 5: Effect of specific dye uptake at different dosages (Chitosan-Selenium nanoparticle) with Rhodamine dye concentration.

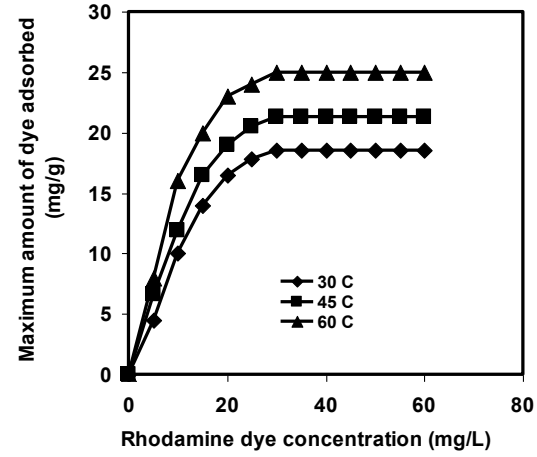

Fig. 6: Effect of specific dye uptake at different temperatures (Chitosan-Selenium nanoparticle) with Rhodamine dye concentration.

uptake. It is obvious that the smaller particles, which have higher solid-liquid interfacial areas, will have higher adsorption rates.Thus dye uptake was maximum at a higher adsorbent dosage. This could be attributed to the fact that as the adsorbent dosage is increased, more adsorption sites are available for dye, thus enhancing the uptake. Also, with increasing adsorbent load, the quantity of dye adsorbed onto the unit weight of the adsorbent gets reduced, thus causing a decrease in q_e value with increasing Chitosan-Selenium nanoparticle loading (Rathinam et al. 2007).

Effect of Temperature

Temperature is an important parameter for the adsorption process. A plot of the Rhodamine dye uptake as a function of temperature (30, 45, and 600°C) is shown in Fig. 6. The results revealed that the dye uptake increased with increasing temperature at 30°C, 16.14 mg/g, 45°C, 24.36.0 mg/g, and 60°C, 25.60 mg/g). The adsorption of dye at higher temperatures was found to be greater compared to that at a lower temperature. The curves indicate the strong tendency of the process for monolayer formation (Sivaraj et al. 2001, Annadurai et al. 2002, Yu et al. 2002, Ravi Kumar 2000,Muzzarelli 1973). The increase in temperature would increase the mobility of the large dye ion and also produces a swelling effect within the internal structure of the Chitosan-Selenium nanoparticle, thus enabling the large dye molecule to penetrate further (Muzzarelli 1973, Faria et al. 2004). Therefore, the adsorption capacity should largely depend on the chemical interaction between the functional groups on the adsorbent surface and the adsorbate and should increase with temperature rising (Rinaudo 2006,Knorr et al.1985, Kawamura et al.1997). This effect is characteristic of a chemical reaction or bond being involved in the adsorption process. The increase in adsorption with temperature could be due to changes in pore size, an increase in kinetic energy of dye molecule, and enhanced rate of diffusion of sorbate (Aksu 2002, Rathinam et al. 2007).

Effect of pH

Fig. 7.showsthe effect of pH on adsorption of the Rhodamine dye onto Chitosan-Selenium nanoparticle. In general, uptakes were much higher in acidic solutions than those in neutral and alkaline conditions. The maximum values of the adsorption capacity ratio between acidic and alkaline conditions reached 12.14 to 19.49 mg/g, respectively. At lower pH more protons will be available to protonate amino groups of chitosan molecules to form groups $–NH^{3+}$, thereby increasing the electrostatic attractions between negatively charged dye anions and positively charged adsorption sites and causing an increase in dye adsorption (Gardiner & Brune 1978, Ganesh et al. 1994, Fu & Viraraghavan 2001, Forgacs et al. 2004). This explanation agrees with our data on the pH effect. It can be seen that the pH of aqueous solution plays an important role in the adsorption of Rhodamine dye onto Chitosan-Selenium nanoparticle. The results showed a direct influence of the pH of the solution on the heterogeneous adsorption process. In alkaline solutions, adsorption efficiency was more than that in acidic solutions. It is because the decomposition of Chitosan- Selenium nanoparticle takes place in acidic and neutral solutions (Daneshvar et al. 2007).

Langmuir Isotherm

The Langmuir isotherm (1916, 1918) has found successful application to many other real sorption processes and it can be used to explain the sorption of Rhodamine dye into

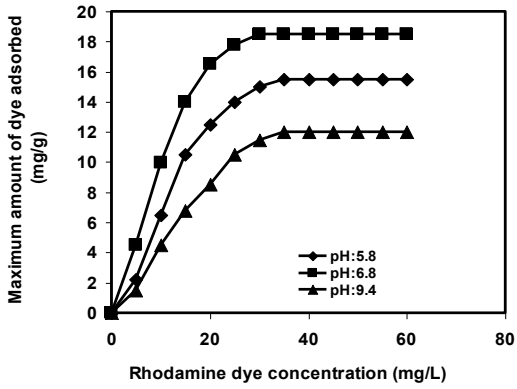

Fig. 7: Effect of specific dye uptake at different pH (Chitosan-Selenium nanoparticle) with Rhodamine dye concentration.

Chitosan-Selenium nanoparticle. A basic assumption of the Langmuir theory is that sorption takes place at specific sites within the adsorbent (Kawamura et al. 1993, Lee& Low 1987, Wei et al.1992). The data obtained from the adsorption experiment conducted in the present investigation were fitted in different Rhodamine dye concentrations, dosages, pH, and temperature in the isotherm equation. The saturation monolayer can be represented by the expression (2).

$$q_e = \frac{KbC_e}{(1+bC_e)} \quad \ldots (2)$$

Linear Regression of Langmuir Isotherm -Chitosan-Selenium Nanocomposite-Rhodamine Dye

A plot of Langmuir isotherm Type – I - IV (C_e/q_e Vs C_e- Type-I. 1/qe vs $1/C_e$ – Type – II. q_e Vs qe/C_e - Type- III. q_e/C_e Vs q_e –Type- IV) (Table1)resulted in a linear graphical relation indicating the applicability of the above model (Different dosage 1.0, 2.0, and 3.0g/L, pH: 5.8, 6.8, and 9.4. Temperature: 30°C, 45°C, and 60°C) as shown in Figs.8-19. The values are calculated from the slope and intercept of different straight lines representing the different dosages, pH, and temperature (q_m) adsorption capacity. The Langmuir isotherm constant (K_L) in Eqn (3 - 7) is a measure of the amount of dye adsorbed when the monolayer is completed. Monolayer capacity (q_m) of the adsorbent for the dye is comparably obtained from adsorption isotherm. The observed statistically significant (at the 95% confidence level) linear relationship as evidence of these by the R^2 values (close to unity) indicate the applicability of the isotherm (Langmuir isotherm) and surface.

The Langmuir isotherm constants along with correction coefficients are reported in Tables2-5.It is also clear from the shape of the adsorption isotherm, that it belongs to the L_2 category of isotherm, which indicates the normal (or) Langmuir type of adsorption (Chiou et al. 2003, Yui et al.1994, Rinaudo 2006, Kurita 2001). Such isotherms are often encountered when the adsorbate has a strong intermolecular attraction for the surface of the adsorbent. The L_2 shape of the isotherm observed in the present care implies that Rhodamine dye molecules must have been strongly attached to the Chitosan-Selenium nanoparticle. Langmuir equation can be written in four linearized types, the Langmuir constants q_m and K_L values can be calculated by plotting between type 1- C_e/q_e versus C_e, type 2 - $1/q_e$ versus $1/C_e$, type 3 - q_e versus q_e/C_e, and type 4q_e/C_e versus q_e, Langmuir isotherms, respectively.

The linear method does not test whether the experimental data are linear. It assumes the experimental data were linear and predicts the slope and intercepts that make a straight line that predicts the best-fit of experimental equilibrium data (Yoshida & Takemori 1997, Gupta et al. 1989, Giunchedi et al. 1998, Ghosh & Bhattacharyya 2002, Gupta et al. 2003). The linear method assumes that the scatter of points around the line follows a Gaussian distribution and the error distribution is the same at every value of *X*. The linear method just predicts the *Y* for the corresponding *X*. It considers only the error distribution

Table 1: The different linearized forms of Langmuir and Freundlich equations.

Isotherm	Linear Regression	Plot
Langmuir Isotherm Type 1- (Eqn-3)	$C_e/q_e = (1/K_L q_m)+(C_e/q_m)$	$C_e \ / \ q_e.vs.C_e$
Langmuir Isotherm Type 2- (Eqn-4)	$1/q_e = (1 \ / \ q_m)+(1 \ / \ K_L q_m C_e)$	$1 \ / \ q_e.vs.1 \ / \ C_e$
Langmuir Isotherm Type 3- (Eqn-5)	$q_e = q_m - (q_e \ / \ K_L C_e)$	$q_e.vs.q_e \ / \ C_e$
Langmuir Isotherm Type 4- (Eqn-6)	$q_e \ / \ C_e = K_L q_m - K_L q_e$	$q_e \ / \ C_e.vs.q_e$
Freundlich Isotherm (Eqn-7)	$Log(C_e) = Log(K_F)+1 \ / \ nLog(C_e)$	$Log(q_e).vs.Log(C_e)$

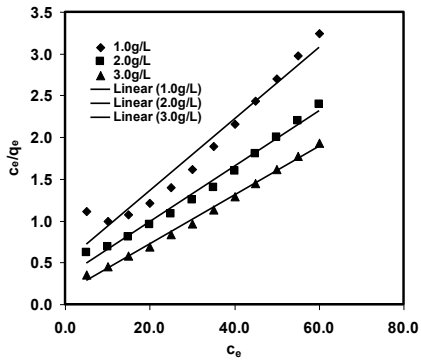

Fig. 8: Langmuir isotherm (Type – I) for the adsorption of Rhodamine dye using Chitosan-Selenium nanocomposite at different Dosages with dye concentration.

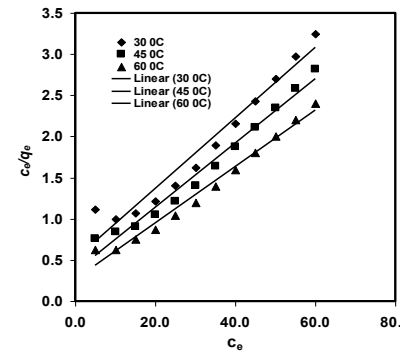

Fig. 9: Langmuir isotherm (Type – I) for the adsorption of Rhodamine dye using Chitosan-Selenium nanocomposite at different Temperatures with dye concentration.

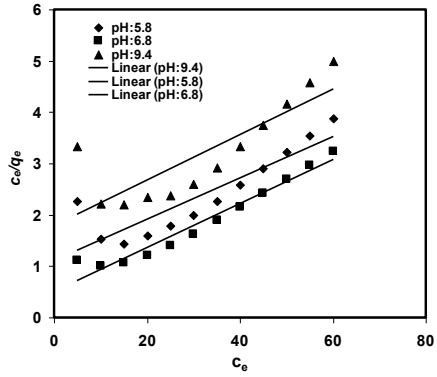

Fig. 10: Langmuir isotherm (Type – I) for the adsorption of Rhodamine dye using Chitosan-Seleniumnanocomposite at different pH with dye concentration.

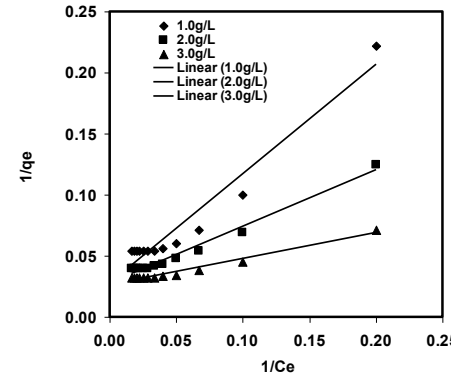

Fig. 11: Langmuir isotherm (Type – II) for the adsorption of Rhodamine dye using Chitosan-Selenium nanocomposite at different Dosages with dye concentration.

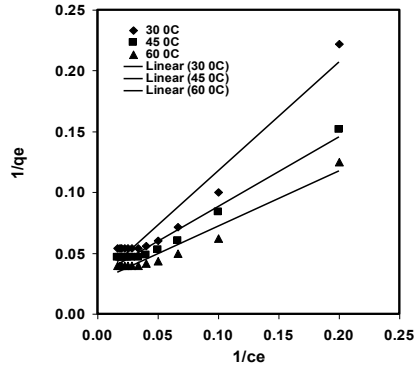

Fig. 12: Langmuir isotherm (Type – II) for the adsorption of Rhodamine dye using Chitosan-Seleniumnanocomposite at different Temperatures with dye concentration.

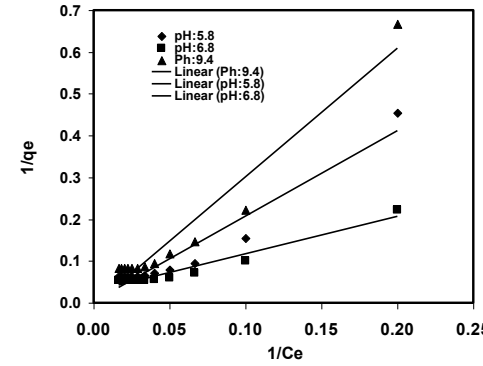

Fig. 13**:** Langmuir isotherm (Type – II) for the adsorption of Rhodamine dye using Chitosan-Selenium nanocomposite at different pH with dye concentration.

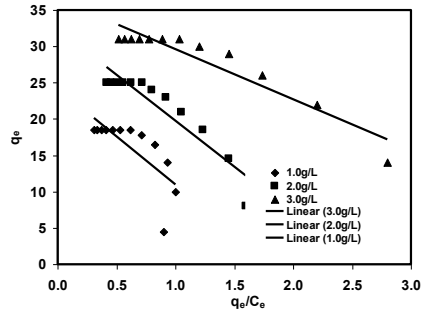

Fig. 14: Langmuir isotherm (Type – III) for the adsorption of Rhodamine dye using Chitosan-Selenium nanocomposite at different Dosages with dye concentration.

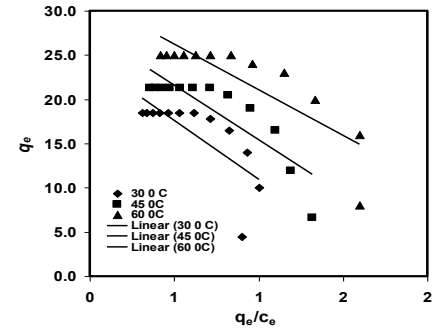

Fig. 15: Langmuir isotherm (Type – III) for the adsorption of Rhodamine dye using Chitosan-Selenium nanocomposite at different Temperatures with dye concentration.

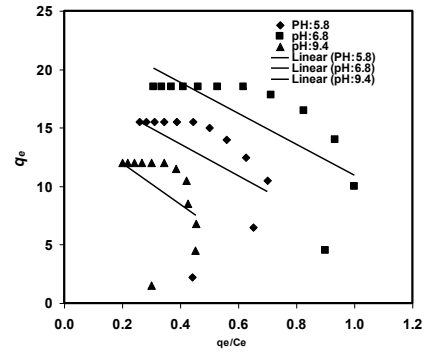

Fig. 16: Langmuir isotherm (Type – III) for the adsorption of Rhodamine dye using Chitosan-Seleniumnanocomposite at different pH with dye concentration.

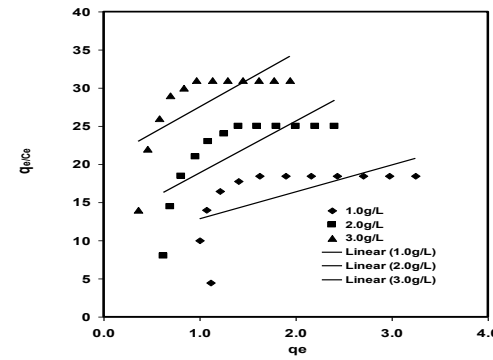

Fig. 17: Langmuir isotherm (Type – IV) for the adsorption of Rhodamine dye using Chitosan-Selenium nanocomposite at different Dosages with dye concentration.

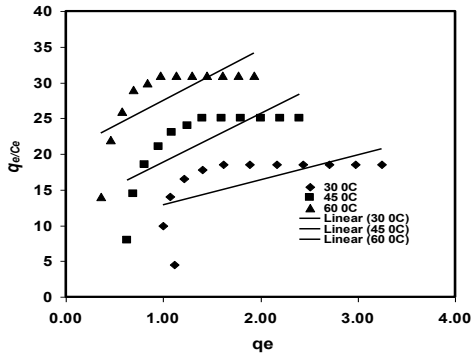

Fig. 18: Langmuir isotherm (Type – IV) for the adsorption of Rhodamine dye using Chitosan-Seleniumnanocomposite at different Temperatures with dye concentration.

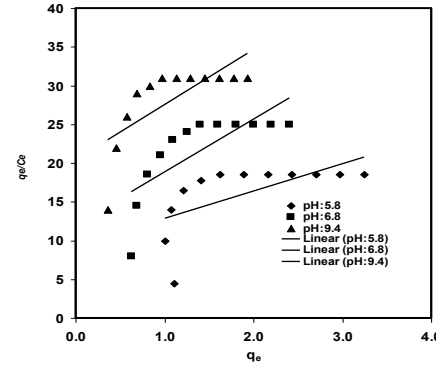

Fig. 19:Langmuir isotherm (Type – IV) for the adsorption of Rhodamine dye using Chitosan-Seleniumnanocomposite at different pH with dye concentration.

along the *Y*-axis irrespective of the corresponding *X*-axis resulting in the different determined parameters.

Freundlich Isotherm- Rhodamine Dye-Chitosan-Selenium Nanoparticle

Freundlich (1906) isotherm is used for the heterogeneous surface energies system. The sorption isotherm is the most convenient form of representing the experimental data at different dosages like Chitosan- Selenium nanoparticle withdosages, pH, and temperature as shown in Fig.20-22.

$$q_e = K_F C_e^{1/n} \quad ...(8)$$

$$\ln q_e = \ln K_F /(1/n) \ln C_e \quad ...(9)$$

The various constants, associated with the isotherm are the intercept, which is roughly on the indicator of sorption capacity (kf), and the slope (1/n) sorption intensity values recorded in Table 2 from Equations 8 and 9. Freundlich isotherm has been illustrated to be a special case of heterogeneous surface energies and it can be easily extended to this case. It has been stated by Krajewska (2005)& Kawamura et al.(1997), that magnitude of the exponent 1/n indicates the favourability and capacity of the adsorbent/adsorbate system. The values n>1 represent favourable adsorption

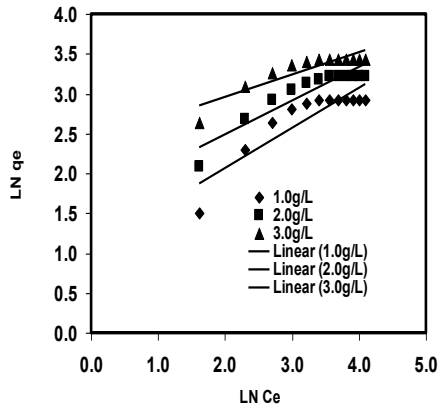

Fig. 20: Freundlich isotherm for the adsorption of Rhodamine dye using Chitosan-Seleniumnanocomposite at different Dosages with dye concentration.

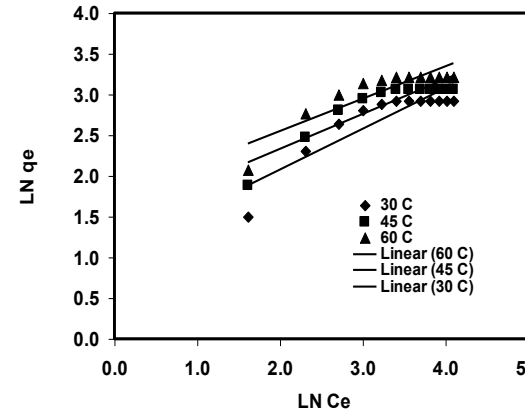

Fig. 21:Freundlich isotherm for the adsorption of Rhodamine dye using Chitosan-Seleniumnanocomposite at different Temperatures with dye concentration.

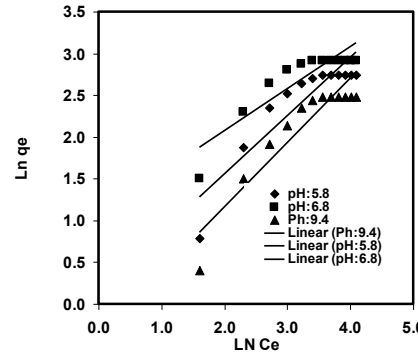

Fig. 22: Freundlich isotherm for the adsorption of Rhodamine dye using Chitosan-Selenium nanocomposite at different pH with dye concentration.

conditions. In most cases, the exponent between 1<n<10 shows beneficial adsorption.

Mechanism of adsorption according to the process of adsorption occurs either in a single step or in the combination of the steps such as film or external diffusion, pore diffusion, surface diffusion, and adsorption on the pore surface. It was also reported that adsorption on the adsorbent surface proceeds in three steps: (1) migration to the surface, (2) dissociation (or deprotonation) of complexes in an aqueous solution. Once equilibrium is attained, the migration of the solute species from the solution stops. Under this situation, it is possible to measure the magnitude of the distribution of the solute species between the liquid and solid phases. The magnitude of this kind of distribution is a measure of the efficiency of the chosen adsorbent in the adsorbate species. When a powdered solid adsorbent material is made in contact with a solution containing dyes, the dyes first migrate from the bulk solution to the surface of the liquid film. This surface exerts a diffusion barrier.

This barrier may be very significant or less significant (Gupta et al. 2005, Karthikeyan et al. 2010). The involvement of a significant quantum of diffusion barrier indicates the dominant role taken up by the film diffusion in the adsorption process. Furthermore, the rate of an adsorption process is controlled either by external diffusion, internal diffusion, or by both types of diffusions. The external diffusion controls

Table 2: Langmuir and Freundlich isotherm constants at different dosages, pH, and temperature(Chitosan- Selenium nanocomposite-Rhodamine dye).

Dosages(g/L)	Langmuir IsothermType - I	Freundlich Isotherm model parameters
1.0 g/L	q_m =2.34. K_L = 0.84. R^2 = 0.9558	K_F = 0. 8011. 1/n = 0.9314. R^2 = 0.8011
2.0 g/L	q_m = 30.21. K_L = 0.10. R^2= 0.9873	K_F = 0.4211. 1/n = 0.6063. R^2 = 0.8640
3.0 g/L	q_m = 34.13. K_L = 0.21. R^2= 0.9952	K_F = 0.2829. 1/n = 0.4185. R^2 = 0.8117
Temperature (°C)	Langmuir Isotherm Type - I	Freundlich Isotherm model parameters
30	q_m = 23.36. K_L = 0.84. R^2= 0.9558	K_F = 0.3953. 1/n = 0.5671. R^2 = 0.7889
40	q_m = 25.58. K_L = 1.00. R^2= 0.9793	K_F = 0.4291. 1/n = 0.6787. R^2 = 0.8253
60	q_m = 29.24. K_L = 1.30. R^2= 0.9829	K_F = 0.5005. 1/n = 0.9314. R^2 = 0.8011
pH	Langmuir Isotherm Type - I	Freundlich Isotherm model parameters
5.8	q_m =22.73. K_L = 0.0245. R^2= 0.6922	K_F = 0.5005. 1/n =6.1843. R^2 = 0.8205
6.8	q_m =25.00. K_L = 0.0359. R^2= 0.7843	K_F = 0.4211. 1/n =0.9314. R^2 = 0.8011
9.4	q_m =23.36. K_L =0.0840. R^2= 0.9558	K_F = 0.2829. 1/n = 2.6247. R^2 = 0.8636

Table 3: Langmuir isotherm constants at different dosages, pH,and temperature (Chitosan-Seleniumnanocomposite-Rhodamine dye).

Dosages (g/L)	Langmuir Isotherm – Type – II
1.0 g/L	q_m = 36.23 . K_L = 0.031 . R^2 = 0.9476
2.0 g/L	q_m = 35.97 . K_L = .060 . R^2= 0.9793
3.0 g/L	q_m = 37.88 . K_L = 0.123 . R^2= 0.9724
Temperature (°C)	Langmuir Isotherm – Type – II
30	q_m = 36.23 . K_L = 0.031 . R^2= 0.9476
40	q_m = 32.63 . K_L = 0.054 . R^2= 0.9693
60	q_m = 37.31 . K_L = 0.059 . R^2= 0.9491
pH	Langmuir Isotherm – Type – II
5.8	q_m = 161.29. K_L = 0.0022 . R^2 = 0.9422
6.8	q_m = 312.50. K_L = 0.0024 . R^2= 0.9301
9.4	q_m = 36.23 . K_L = 0.031 . R^2= 0.9476

Table 4: Langmuir constants at different dosages, pH, and temperature (Chitosan-Selenium nanocomposite- Rhodamine dye).

Dosages (g/L)	Langmuir Isotherm – Type – III
1.0 g/L	q_m = 36.48 . K_L = 0.15 . R^2 = 0.8894
2.0 g/L	q_m = 32.48 . K_L = 0.087 . R^2= 0.8656
3.0 g/L	q_m = 24.20 . K_L = 0.082 . R^2= 0.5551
Temperature (°C)	Langmuir Isotherm – Type – III
30	q_m = 24.20. K_L = 0.08 . R^2= 0.5511
40	q_m = 27.73. K_L = .08 . R^2= 0.7468
60	q_m = 31.33. K_L = 0.10 . R^2= 0.7114
pH	Langmuir Isotherm – Type – III
5.8	q_m = 19.05 . K_L = 0.07 . R^2= 0.2210
6.8	q_m = 13.25 . K_L = 0.08 . R^2= 0.5511
9.4	q_m = 17.50 . K_L = 0.06 . R^2= 0.2039

the migration of the solute species from the solution to the boundary layer of the liquid phase. However, the internal diffusion controls the transfer of the solute species from the external surface of the adsorbent to the internal surface of the pores of the adsorbent material (Karthikeyan et al. 2010 and Gupta et al. 2003b). It is now well established, that during the adsorption of dye over a porous adsorbent, the following three consecutive steps were taken place (Crank 1975 and Karthikeyan et al. 2010) (i) Transport of the ingoing adsorbate ions to the external surface of the adsorbent (film diffusion), (ii) Transport of the adsorbate ions within the pores of the adsorbent except for a small amount of adsorption, which occurs on the external surface (particle diffusion) and (iii) Adsorption of the ingoing adsorbate ions on the interior surface of the adsorbent (Weber & Morris 1963 and Karthikeyan et al. 2010).

CONCLUSION

In this study, the ever-increasing problem of dye pollutants and ways of dye remediation has been discussed. The environment-friendly technique of adsorption is brought

Table 5: Langmuir constants at different dosages, pH, and temperature (Chitosan-Selenium nanocomposite-Rhodamine dye).

Dosages (g/L)	Langmuir Isotherm – Type – IV
1.0 g/L	q_m = -2.64 . K_L = -3.5255. R^2= 0.3889
2.0 g/L	q_m = -1.77 . K_L = -6.8158 . R^2= 0.5725
3.0 g/L	q_m = -2.89 . K_L = -7.0853 . R^2= 0.5082
Temperature (°C)	Langmuir Isotherm – Type – IV
30	q_m = -2.64 . K_L = -3.525 . R^2= 0.3889
40	q_m = -2.46 . K_L = -4.545 . R^2= 0.4655
60	q_m = -2.56 . K_L = -5.625 . R^2= 0.4445
pH	Langmuir Isotherm – Type – IV
5.8	q_m = -2.64 . K_L = -3.5255 . R^2= 0.3889
6.8	q_m = -1.77 . K_L = -6.8185 . R^2= 0.5725
9.4	q_m = -2.89 . K_L = -7.0852 . R^2= 0.5082

into the light. The enhanced properties of the nanomaterials because of their small size and ways of synthesizing them have been summed up. The plant *Justicia adhatoda* leaf extract is used to produce Chitosan-Selenium nanocomposite which acts as good reducing agents for the preparation of Chitosan-Selenium nanocomposite. Likewise, chitosan–selenium nanocomposite was prepared by a simple step. UV-. Vis spectra show characteristics peak for Chitosan-Selenium nanocomposite. XRD shows the crystalline structure of Chitosan-Selenium nanocomposite, whereas the amorphous structure of chitosan-selenium nanocomposite indicates chitosan strongly coated with selenium nanoparticles. FTIR shows that functional groups responsible for the synthesis of the process are phenols, carboxylic acid, primary amine and nitro compounds, etc. for both nanoparticles. The average particle size range was noted for Chitosan-Selenium nanocomposite as 87-152 nm, respectively. Adsorption depends upon the chemical nature of the material, various physicochemical experimental conditions such as solution pH, adsorbent dosage, temperature. Adsorption technology provides an attractive pathway for further research and improvement in more efficient nanoparticles, with higher adsorption capacity, for numerous dyes to eliminate the dyes discharged from various industries and thus reduce the contamination of water.

REFERENCES

Aksu, Z. 2002.Determination of the equilibrium, kinetic and thermodynamic parameters of the batch biosorption of nickel(II) ions onto *Chlorella vulgaris.* Process Biochemistry, 38(1): 89-99.

Alkan, M. and Dogan, M. 2001. Adsorption of copper (II) onto perlite. J. Colloid Interf. Sci., 243(2): 280-291.

Allen, S. J., Mckay, G. and Khader, K. Y. H. 1989. Equilibrium adsorption isotherms for basic dyes onto lignite. J. Chem. Technol. Biotechnol., 45: 291-302.

Annadurai, G., Juang, R.S. and Lee, D.J. 2002. Use of cellulose-based wastes for adsorption of dyes from aqueous solutions. J. Hazard. Mater., **B92,** 263-74.

Arica, T.A., Ayas, E. and Arica, M.Y. 2017. Magnetic MCM-41 Silica particles grafted with poly (glycidyl methacrylate) brush: modification and application for removal of direct dyes. Microporous and Mesoporous Materials, 243(1): 164-175.

Arica, T.A., Kuman, M., Gercel, O. and Ayas, E. 2019. Poly (dopamine) grafted bio-silica composite with tetraethylenepentamine ligands for enhanced adsorption of pollutants. Chemical Engineering Research and Design, 141: 317-327.

Ashraf, M.W. 2016. Removal of methylene blue dye from wastewater by using supported liquid membrane technology. Polish Journal of Chemical Technology, 18(2): 26-30.

Baba, I.M., Lai, P. and Yifeng, X. 2020. Adsorption of methylene blue using chemically enhanced *Platanus orientalis*leaf powder: kinetics and mechanisms. Nature Environment and Pollution Technology, 9(1): 29-40.

Bajaj, M., Schmidt, S. and Winter, J. 2012. Formation of Se (0) Nanoparticles by *Duganellasp* and *Agrobacterium sp*. isolated from Se-laden soil of North-East Punja India. Microbial Cell Factories,11(1).

Bayramoglu, G. and Yilmaz, M. 2018. Azo dye removal using free and immobilized fungal biomasses: Isotherms, kinetics, and thermodynamic studies. Fibers and Polymers, 19(4): 877-886.

Bayramoglu, G., Altintas, B. and Arica, M.Y. 2012. Synthesis and characterization of magnetic beads containing aminated fibrous surfaces for removal of Reactive Green 19 dye: Kinetics and thermodynamic parameters. Journal of Chemical Technology & Biotechnology, 87(5): 705-713.

Bereket, G., Arogus, A.Z. and Ozel, M. Z. 1997. Removal of Pb (II), Cd (II), Cu (II) and Zn (II) from aqueous solutions by adsorption on bentonite. J. Colloid Interf. Sci., 187(2): 338-343.

Chang, K.L., Chen, C. C., Lin, J., Hsien, J.F., Wang, Y., Zhao, F., Shih, Y.H., Xing, Z.J. and Chen, S.T. 2014. Rice straw-derived activated carbons for the removal of carbofuran from an aqueous solution. New Carbon Materials, 29(1): 47-54.

Chiou, M.S. and Li, H.Y. 2003. Adsorption behaviour of reactive dye in aqueous solution on chemical cross-linked chitosan beads. Chemosphere, 50: 1095.

Crank, J. 1975. The Mathematics of Diffusion, 2nd Ed. Clarendon, Oxford.

Daneshvar, N., Rasoulifard, M.H., Khataee, A.R. and Hosseinzadeh, F. 2007. Removal of C.I. Acid Orange 7 from aqueous solution by UV irradiation in the presence of ZnOnanopowder. Journal of Hazardous Materials, 143: 95-10.1

Demirbas, O. and Dogan, M. 2002. The removal of Victoria blue from aqueous solution by adsorption on a low-cost material. Adsorption, 8: 341-349.

Dogan, M. and Alkan, M. 2003. Adsorption kinetics of methyl violet onto perlite. Chemosphere, 50: 517-528.

Dogan, M. and Alkan, M. 2003. Adsorption kinetics of Victoria blue onto perlite. Fresenius Environ. Bull., 12(5): 418-425.

Dogan, M. and Alkan, M. 2003. Removal of methyl violet from aqueous solution by perlite. J. Colloid Interf. Sci., 267: 32-41.

Dogan, M., Alkan, M. and Onganer, Y. 2000. Adsorption of methylene blue from aqueous solution onto perlite. Water Air Soil Pollut., 120: 229-248.

El-Sharkawy, E.A., Soliman, A.Y. and Al-Amer, K.M. 2007. Comparative study for the removal of methylene blue via adsorption and photocatalytic degradation. J. Colloid Interface Sci., 310: 498-508.

Eren, E. and Afsin, B. 2007. Investigation of a basic dye adsorption from aqueous solution onto raw and pre-treated sepiolite surfaces. Dyes and Pigments, 73(2): 162-167.

Faria, P.C.C., Orfao, J.J.M. and Pereira, M.F.R. 2004. Adsorption of anionic and cationic dyes on activated carbons with different surface chemistries. Water Res., 38: 2043-2052.

Feng, C.W., Ru, L.T. and Juang, R.S. 2001. Kinetic modeling of liquid-phase adsorption of reactive dyes and metal ions on chitosan. Water Research, 35: 613-18.

Ferrero, F. 2000. Oxidative degradation of dyes and surfactant in the Fenton and Photo-Fenton treatment of dye house effluentscolor. Technol., 116: 148-153.

Fesharaki, P.J., Nazari, P., Shakibaie, M., Rezaie, S.M., Banoee, S., Abdollahi, M. and Shahverdi, A.R. 2010. Biosynthesis of selenium nanoparticles using *Klebsiella pneumoniae* and their recovery by a simple sterilization process. Brazilian Journal of Microbiology, 41: 1517-8382.

Forgacs, E., Cserhati, T. and Oros, G. 2004. Removal of synthetic dyes from wastewater: A review. Environ. Int., 30: 953-971.

Freundlich, H.M.F. 1906. Uber die adsorption in losungen. ZeitschriftPhysikalischeChemie, 57: 385-470.

Fu, Y. and Viraraghavan, T. 2001. Fungal decolorization of wastewaters: A review. Bioresource Technol., 79: 251-262.

Ganesh, R., Boardman, G.D. and Michelsen, D. 1994. Fate of azo dye in sludges. Water Res., 28(13): 67-76.

Gardiner, D.K. and Brune, B.J. 1978. Textile wastewater treatment and environmental effects. J.Soc. Dyers and Colorists, 94: 339-348.

Ghosh, D. and Bhattacharyya, K.G. 2002. Adsorption of methylene blue on Kaolinite. Appl. Clay Sci., 20: 295-300.

Giunchedi, P., Genta, I., Conti, B., Muzzarelli, R.A.A. and Conte, U. 1998. Preparation and characterization of ampicillin loaded methylpyrrolidinone chitosan and chitosan microspheres. Biomaterials, 19: 157-161.

Gupta, G.S., Prasad, G., Panday, K.K. and Singh, V.N. 1989. Removal of chrome dye from aqueous solution by fly ash. Water Soil. Pollut., 37: 13-24.

Gupta, V. K., Ali, I. Suhas and Mohan, D. 2003. Equilibrium uptake and sorption dynamics for the removal of a basic dye (basic red) using low-cost adsorbents. J. Colloid Interface Sci., 265: 257-264.

Gupta, V. K., Mittal, A. and Gajbe, V. 2005. Adsorption and desorption studies of a water-soluble dye, Quinoline Yellow, using waste materials. J. Colloid Interface Sci., 284: 89-98.

Gupta, V. K., Mohan, D., Sharma, S. and Sharma, M. 2000. Removal of basic dye (rhodamine-B and methylene blue) from aqueous solution using bagasse fly ash. Sep. Sci. Technol., 35(13): 2097.

Hamza, A. and Hamoda, M.F. 1980. Multiprocess treatment of textile wastewater. In: Proceedings of the 35th Industrial Waste Conference, Purdue University, Lafayette, Indiana, p.151.

Ho, Y. S. and Mckay, G. 1998. Sorption of dye from aqueous solution by peat. Chem. Eng. J., 70(2): 115-124.

Jain, A.K., Gupta, V.K., Bhatnagar, A. and Suhas 2003. Utilization of industrial waste products as adsorbents for the removal of dyes. Journal of Hazardous Material B, 101: 31-42.

Janos, P., Buchtova, H. and Rýznarova, 2003. Sorption of dyes from aqueous solutions onto fly ash. Water Research, 37(20): 4938-4944.

Jumasiah, A., Chuah, T.G., Gimbon, J., Choong, T.S.Y. and Azni, I. 2005. Adsorption of basic dye onto palm kernel shell activated carbon: sorption equilibrium and kinetics studies. Desalination, 186: 57-64.

Kadirvelu, K., Karthika, C., Vennilamani, N. and Pattabhi, S. 2005. Activated carbon from industrial solid waste as an adsorbent for the removal of Rhodamine-B from aqueous solution: Kinetic and equilibrium studies. Chemosphere, 60: 1009-1017.

Kamel, D., Sihem, A., Halima, C. and Tahar, S. 2009. Decolourization process of an azoique dye (Congo red) by photochemical methods in homogeneous medium. Desalination, 247: 412-422.

Karthikeyan, S., Sivakumar, B. and Sivakumar, N. 2010. Film and pore diffusion modeling for adsorption of Reactive Red 2 from aqueous solution on to activated carbon prepared from bio-diesel industrial waste. E-Journal of Chemistry, 7(1): 175-184.

Kaushik, P. and Malik, A. 2009. Fungal dye decolorization: Recent advances and future potential. Environ. Int., 35: 127-141.

Kawamura, Y., Mitsuhashi, M., Tanibe, H. and Yoshida, H. 1993. Adsorption of metal ions on polyaminated highly porous chitosan chelating resin. Ind. Eng. Chem. Res., 32: 386-391.

Kawamura, Y., Yoshida, H. and Asai, S. 1997. Effects of chitosan concentration and precipitation bath concentration on the material properties of porous crosslinked chitosan beads. Sep. Sci. Technol., 32: 1959-1974.

Kirupagaran, R., Saritha, A. and Bhuvaneswari, S. 2016. Green synthesis of selenium nanoparticles from leaf and stem extract of Leucaslavandulifolia Sm. and their application. J.Nanosci. Tech., 2(5): 224–226.

Knorr, D. 1985. Food technology. In: R.R. Colwell, E.R. Pariser and A.J. Sinskey (Ed.), Biotechnology of Marine Polysaccharides, Vol. 85, Hemisphere, New York. p. 313.

Krajewska, B. 2005. Membrane-based processes performed with use of chitin/chitosan materials Sep. Purif. Technol., 41: 305-312.

Kurita, K. 2001. Controlled functionalization of polysaccharide chitin. Progress in Polymer Science, 26(9): 1921-1971.

Langmuir, I. 1916. The constitution and fundamental properties of solids and liquid. J. Am. Chem. Soc., 38(11): 2221-2295.

Langmuir, I.J. 1918. The adsorption of gases on plane surface of glass, mica, and platinum. J. Chem.Soc., 40: 1361-1366.

Lee, C.K. and Low, K.S. 1987. The removal of cationic dyes by a natural moss 1-adsorption studies. Pertanika, 10: 327-334.

Lin, Z.H. and Wang, C.R.C. 2005. Evidence on the size-dependent absorption spectral evolution of selenium nanoparticles. Mater. Chem. Phys., 92: 591-594.

Mall, I. D., Srivastava, V. C., Agarwal, N. K. and Mishra, I. M. 2005. Adsorptive removal of malachite green dye from aqueous solution by bagasse fly ash and activated carbon-kinetic study and equilibrium isotherm analyses. Colloids and Surfaces A, 264(1-3): 17-28.

Mallikarjuna, K., Narasimha, G., Dillip, G.R., Praveen, B. and Shreedhar, B. 2011. Green synthesis of silver nanoparticles using *Ocimum* leaf extract and their characterization. Dig. J. Nanomat. Biostruc,. 6: 181-186.

McKay, G. 1980. Color Removal by Adsorption. American Dye-stuff Reports, p. 38.

Mckay, G. 1984. Analytical solution using a pore diffusion model for a pseudo-irreversible isotherm for the adsorption of basic dye on silica. AICHE J., 30: 692.

Mckay, G. M.S. and Otterburn, A.G. 1981. Sweeney, Surface mass transfer processes during colour removal from effluent using silica. Water Res., 15: 327-331.

Mohamed, M.M. 1996. Adsorption properties of ionic surfactants on molybdenum-modified silica gels. Colloid Surf. A: Physicochem. Eng. Aspects, 108: 39-48.

Mohan, D., Singh, K.P. and Kumar, K. 2002. Removal of dyes from wastewater using fly ash, a low-cost adsorbent. Ind. Eng. Chem. Res., 42: 1965-1976.

Muzzarelli, R.A.A. 1973. Natural Chelating Polymers, Pergamon Press, Oxford.

Nurchi, V. M. M. Crespo-Alonso, and Biesuz, R. 2014. Sorption of chrysoidine by row cork and cork entrapped in calcium alginate beads. Arabian Journal of Chemistry, 138-133 :(1)7.

Oliveira, L.S., Franca, A.S., Alves, T.M. and Rocha, S.D.F. 2008. Evaluation of untreated coffee husks as potential biosorbents for treatment of dye contaminated waters. J. Hazard. Mater., 155: 507-512.

Ramamurthy, C.H., Sampath, K.S., Arunkumar, P., Suresh Kumar, M., Sujatha, V. and Premkumar, K. Thirunavukkarasu, C. 2013. Green synthesis and characterization of selenium nanoparticles and its augmented cytotoxicity with doxorubicin on cancer cells. Bioprocess Biosyst. Eng., 36: 1131-1139.

Rathinam, A., Nishtar, N. F., Jonnalagadda, R. and Balachandran, U. 2007. Equilibrium and thermodynamic studies on the removal of basic black dye using calcium alginate beads. Colloids and Surfaces A: Physicochem. Eng. Aspects, 299: 232-238.

Ravi Kumar, M.N.V. 2000. A review of chitin and chitosan applications. React. Funct. Polym., 46: 1-27.

Rinaudo, M. 2006. Characterization and properties of some polysaccharides used as biomaterials. Macromol. Sympl., 245-246: 549-557.

Senthilkumar, S.R. and Sivakumar, T. 2014. Green tea (Camellia sentences) mediated synthesis of zinc oxide (ZnO) nanoparticles and studies on their antimicrobial activities. Inter. J. Pharm. Pharm. Sci., 6: 461-465.

Shaul, G.M., Barnett, M.W. and Dostal, K.A. 1982. Treatment of dye and pigment processing wastewater by activated sludge process. In Proceedings of the 37th Industrial Waste Conference, Purdue University, Lafayette, Indiana, p. 677.

Shelley, M.L., Randall, C.W. and King, P.H. 1976. Evaluation of chemical-biological and chemical physical treatment for textile dyeing and finishing waste. J. WPCF, 4: 753.

Shen, Y., Xiufang, W., Xie, A., Huang, L. and Zhu, J. 2000. Synthesis of dextran/Se nanocomposites for nanomedicine application. Mater. Chem. Phys., 109: 534-540.

Sivaraj, R., Namasivayam, C. and Kadirvelu, K. 2001. Orange peel as an adsorbent in the removal of Acid Violet 17 (Acid Dye) from aqueous solutions. Waste Manag., 21: 105.

Wang, Z., Xue, M., Huang, K. and Liu, Z. 2011. Textile dyeing wastewater treatment. Advances in Treating Textile Effluent, 5: 91-116.

Weber, W. J. and Morris, C. J. 1963. Kinetics of adsorption on carbon from solution. J. Sanit. Eng. Div., 89: 31-60.

Wei, Y.C., Hudson, S.M., Mayer, J.M. and Kaplan, D.L. 1992. The crosslinking of chitosan fibers. J. Polym. Sci. Polym. Chem., 30: 2187.

Yoshida, H. and Takemori, T. 1997. Adsorption of direct dye on cross-linked chitosan fibre: Breakthrough curve. Water Sci. Technol., 35: 29-37.

Yu, M.C., Skipper, P.L., Tannenbaum, S.R., Chan, K.K. and Ross, R.K. 2002. Arylamine exposures and bladder cancer risk. Nutat. Res. Fund. Mol. M., 21: 506-507.

Yui, T., Imada, K., Okuyama, K., Obata, Y., Suzuki, K. and Ogawa, K. 1994. Molecular and crystal structure of the anhydrous form of chitosan. Macromolecules, 27: 7601-7605.